Regulation and modulation of growth : insights from human and animal studies

Gool, S.A.van

Chapter 6

Human fetal mesenchymal stem cells differentiating towards chondrocytes display a similar gene expression profile as growth plate cartilage

S.A. van Gool[1*], J.A.M. Emons[1*], J.C.H. Leijten[2], E. Decker[3], X. Yu[4], C. Sticht[4], J.C. van Houwelingen[5], J.J. Goeman[5], C. Kleijburg[6], S. Scherjon[6], N. Gretz[4], J.M. Wit[1], G. Rappold[3], M. Karperien[1,2].

[1]Department of Pediatrics; [5]Department of Medical Statistics and Bioinformatics, and [6]Department of Obstetrics, Leiden University Medical Center, Leiden, the Netherlands.
[2]Department of Tissue Regeneration, Twente University, Enschede, the Netherlands. [3]Department of Human Molecular Genetics, and [4]Medical Research Center, Medical Faculty Mannheim, University of Heidelberg, Heidelberg, Germany;
[*]These authors contributed equally to this work

Submitted for publication

Abstract

Background: Most studies on growth plate (GP) maturation and fusion have been carried out in animal models not fully representing the human epiphyseal GP.

Aims and methods: We used human fetal bone marrow-derived mesenchymal stem cells (hfMSCs) differentiating towards chondrocytes as an alternative model for the human GP. Our aims were to assess whether chondrocytes derived from hfMSCs are a suitable model for the GP and to study gene expression patterns associated with chondrogenic differentiation.

Results: hfMSCs efficiently formed hyaline cartilage in a pellet culture in the presence of TGFβ3 and BMP6. Microarray and principal component analysis were applied to study gene expression profiles during chondrogenic differentiation. A set of 315 genes was found to correlate with *in vitro* cartilage formation. Several identified genes are known to be involved in cartilage formation and validate the robustness of the differentiating hfMSC model. Other genes like Bradykinin and IFN-γ signaling, CCL20, and KIT were not described in association with chondrogenesis before. KEGG pathway analysis using the 315 genes revealed 9 significant signaling pathways correlated with cartilage formation.

To determine which type of hyaline cartilage was formed, we compared the gene expression profile of differentiating hfMSCs with previously established expression profiles of human articular (AC) and epiphyseal GP cartilage. As differentiation towards chondrocytes proceeds, hfMSCs gradually obtain a gene expression profile resembling epiphyseal GP cartilage, but not AC.

Conclusion: This study validates differentiating bone marrow-derived hfMSCs as an alternative model for the human epiphyseal GP.

Introduction

Growth of the long bones is the result of a tightly orchestrated proliferation and differentiation program called endochondral ossification. In the epiphyseal growth plate of long bones, chondrocytes originating from mesenchymal stem cells subsequently undergo proliferation, hypertrophic differentiation, and programmed cell death before being replaced by bone. At the time of sexual maturation, growth first increases but at the end of puberty epiphyseal fusion and termination of growth occur. Our knowledge on the molecular mechanisms underlying human growth regulation during puberty is limited, although estrogen has been identified as a key regulator of growth plate maturation and fusion (1). Gaining a detailed understanding of growth regulatory processes is essential to facilitate the development of novel strategies for the treatment of various growth disorders.

Commonly used animal models for studying growth plate regulation do not fully represent the human epiphyseal growth plate. For example, rodent growth plates do not fuse at the end of sexual maturation (2), and therefore do not display an important hallmark of human growth plate development. The shortcoming of the mouse model is furthermore demonstrated by the contrast between the marginally affected growth phenotype of the estrogen receptor alpha (ERα) knock out mouse (αERKO) (3) and the prominent growth phenotype of a male patient lacking functional ERα (4), which is characterized by the absence of epiphyseal fusion and continuation of growth into adulthood.

The lack of representative animal models has led to the realization that alternative human models are essential to elucidate the mechanisms involved in growth plate regulation and fusion. However, human growth plate specimens are difficult to obtain, whereas *in vitro* models such as chondrosarcoma cell lines or articular cartilage-derived chondrocyte cultures have limited differentiation capacity, are often difficult to maintain under laboratory conditions or tend to dedifferentiate. Furthermore, articular cartilage and growth plate cartilage have distinct functions and it is therefore questionable whether articular cartilage-derived chondrocytes are representative for epiphyseal growth plate chondrocytes.

Multipotent human mesenchymal stem cells (hMSCs) are a promising *in vitro* model to study chondrogenesis. They have been postulated as an alternative cell source for articular cartilage reconstruction and for studying endochondral ossification as it occurs in the epiphyseal growth plate (5). In this study, we explored the cartilage forming capacity of human fetal (hf)MSCs aiming at the development of an *in vitro* model for the human growth plate. We have chosen human fetal bone marrow-derived MSC for their superior differentiation characteristics compared to adult bone marrow-derived MSCs (6). Efficient cartilage formation was

demonstrated by immunohistochemical analysis and gene expression profiling was applied to identify genetic pathways involved in the differentiation process. In addition, the gene expression profiles of the differentiating hfMSCs were compared with global gene expression patterns of human articular and growth plate cartilage to assess whether differentiating hfMSCs represent either articular or growth plate chondrocytes.

Experimental Procedures

Cell culture

The use of human fetal material was approved by the medical ethical committee of the Leiden University Medical Center and an informed consent was obtained from the women undergoing elective abortion. Cell suspensions of fetal bone marrow were obtained by flushing the long bones of fetuses with M199 washing medium. For the chondrogenic differentiation and microarray analysis, cells derived from a single 22 weeks old fetus were used. MSCs derived from other fetuses were also stimulated to undergo chondrogenic differentiation. Red cells were depleted by incubation for 10 minutes in NH_4Cl (8.4 g/L)/$KHCO_3$ (1g /L) buffer at 4°C. Mononuclear cells were plated at a density of 16×10^4 cells/cm² in M199 culture medium (Gibco) supplemented with 10% fetal bovine serum (FBS), 1% penicillin/streptavidin (P/S), fungizone, endothelial cell growth factor (ECGF) 20 μg/ml (Roche Diagnostics) and heparin 8 U/ml in culture flasks coated with 1% gelatin according to previously established culture conditions for human fetal MSCs (7). Cultures were kept in a humidified atmosphere at 37°C with 5% CO2. The culture medium was changed twice per week. After reaching near-confluence at passage 4 to 5 (15 population doublings), hfMSCs were harvested by treatment with 0.5 % trypsin and 0.5% ethylene diamine tetra acetic acid (EDTA; Gibco) for 5 minutes at 37°C and replated for chondrogenic differentiation.

In vitro chondrogenic differentiation

hfMSCs (2×10^5 cells/well) were cultured in cell pellets. Pellets were formed by centrifugation of the cells at 1200 rpm for 4 minutes in U-shaped 96-well suspension culture plates (Greiner). To induce chondrogenesis the pellets were cultured at 37°C with 5% CO_2 in 200 μl of serum-free chondrogenic medium consisting of high-glucose (25 mM) Dulbecco's modified Eagle's medium (DMEM; Gibco) supplemented with 40 μg/ml proline (Sigma), 100 μg/ml sodium pyruvate (Sigma, USA), 50 mg/ml ITS (insulin-transferrin-selenic acid) with Premix (BD Biosciences), 1% Glutamax (Gibco), 1% penicillin/streptavidin, 50 μg/ml ascorbate-2-phosphate (Sigma), 10^{-7} M

dexamethasone (Sigma), 10 ng/ml transforming growth factor-β3 (TGF-β3; R&D Systems), 500 ng/ml bone morphogenetic protein 6 (BMP6) and antibiotic and antimycotic mix (0.06% polymixin, 0.2% kanamycin, 0.2% penicillin, 0.2% streptavidin, 0.02% nystatin and 0.5% amfotericin essentially as described by Sekiya *et al.*, 2001. The medium was changed twice per week for 5 weeks.

Histological analysis

Two pellets per time point (after 1, 2, 3, 4, or 5 weeks of chondrogenesis) were used for histological evaluation. Pellets were fixed in 10% formalin, dehydrated by treatment with graded ethanols and processed for paraffin embedding. 5 μm sections were cut using a Reichert Jung 2055 microtome (Leica). For each pellet, only the sections from exactly the center of the pellets were mounted on glass slides. Before histological (toluidine blue) or immunohistochemical staining, sections were deparaffinized in xylene, treated with graded ethanols followed by three washing steps with phosphate buffered saline (PBS).
For immunofluorescence of collagen type II, sections were pre-treated with 10mM citric acid buffer (pH=6) for antigen retrieval. Sections were incubated with a collagen type II monoclonal antibody (clone 3HH1-F9, Abnova) at 1:100 dilution in 1% bovine serum albumine (BSA) /PBS buffer overnight at 4°C. After washing, sections were incubated with Alexa Fluor 488-Goat anti-Mouse IgG1 (Invitrogen, Molecular Probes, diluted 1:1000 in PBS/1% BSA) for 1 hour and protected from light. Sections were counterstained with DAPI and mounted with vectashield.
For collagen type X immunohistochemistry, sections were preincubated with blocking buffer (1% H2O2 in 40% methanol, 60% tris buffered saline) twice for 15 minutes at room temperature, followed by overnight incubation at 4°C with mouse monoclonal antibody against collagen type X in a 1:100 dilution (Quartett). Next, sections were incubated with the secondary antibody biotinylated rabbit-anti-mouse IgG (DAKO) in a 1:300 dilution, followed by incubation with horseradish-peroxidase-conjugated-streptavidine (Amersham Biosciences). Staining was visualized with 3-amino-9-ethylcarbazole substrate in 0.2 mg/ml acetate buffer (pH 5.2) with 0.04% H_2O_2. After counterstaining with hematoxylin, the sections were mounted in Histomount (National Diagnostics). Pictures of the stained pellets were taken with a Nikon DXM 1200 digital camera using standardized settings.

RNA isolation

Total RNA from $2 \cdot 10^6$ undifferentiated hfMSCs derived from the 22-weeks old fetus was extracted with Trizol (Invitrogen). After 1, 2, 3, 4, or 5 weeks of chondrogenesis, 60 pellets (per time point) were pooled and homogenized in 1ml 4M guanidine isothiocyanate solution (Sigma) and RNA was extracted according to the optimized method for RNA extraction from cartilage as described by Heinrichs *et al.* (8). The extracted total RNA was purified using the RNeasy kit according to recommendations of the manufacturer (Qiagen).

Gene expression profiling

High RNA quality was confirmed by capillary electrophoresis on an Agilent 2100 bioanalyzer (Agilent). Total RNA (100 ng) was amplified and labeled using the GeneChip Two-Cycle cDNA Synthesis Kit (Affymetrix) and the MEGAscript T7 Kit (Ambion). For gene expression profiling, labeled cRNA was hybridized in duplicate to Affymetrix Human Genome U133 PLUS 2.0 Array Genechips. All procedures were carried out according to the manufacturer's recommendations. Raw data from Affymetrix CEL files were analyzed using SAS software package Microarray Solution version 1.3 (SAS Institute). Custom CDF version 10 with Entrez based gene definitions (9) was applied to map the probes to genes. Gene annotation was obtained using the Affymetrix NetAffx website (http://www.affymetrix.com/analysis/index.affx). Quality control, normalization and statistical modeling were performed by array group correlation, mixed model normalization and mixed model analysis respectively. The normalized expression values for each gene were standardized by linearly scaling the values across all samples of the time course to a mean of 0 with an SD of 1. Analysis of differential gene expression was based on log-linear mixed model of perfect matches (10). A false discovery rate of a=0.05 with Bonferroni-correction for multiple testing was used to set the level of significance. The raw and normalized data are deposited in the Gene Expression Omnibus database (available at http://www.ncbi.nlm.nih.gov/geo).

Microarray data analysis

The statistical analysis of the microarray data was based on the normalized mean expression values per probe at 6 time points with 2 replications at each time point (12 observations per probe). In order to identify subgroups of probes with similar expression profiles over time, a principal component analysis (PCA) of the covariance matrix was carried out on the mean expression value for each probe at each time point. For each probe, factor scores for principal

components 1, 2 and 3 were obtained by regression analysis of the 12 array results (6 time points in duplicate) for that specific probe to those components. The first principal component corresponded with the general expression level during the whole experiment, whereas the second and third component corresponded with changes over time. Since our interest was to identify genes associated with the changes that occur during differentiation from stem cells towards chondrocytes, we focused our analysis on the second and third component. By construction, these factor scores had a mean of 0 with an SD of 1. Generally, the distribution over the factor scores showed a normal distribution with outliers. We used a cut-off of ±3.29 to select outlying probes. This cut-off would select 0.1% of the probes, if the factors scores would follow a pure normal distribution that could be expected if the data were pure noise. The presence of replications allowed us to assess the statistical significance of the factor scores and to remove probes that were not significant at the α=5% level.
In a separate study we compared the gene expression profiles of human articular cartilage (AC) and epiphyseal growth plate (GP) cartilage. A set of 1818 significant differentially expressed genes was identified, that can be used to discriminate between the two hyaline cartilage subtypes (Leijten *et al.*, manuscript in preparation). All AC (n=5) and GP (n=5) samples were derived from 9 to 17 year old female donors with no history of growth disorders. The gene expression profiles of the stem cells differentiating towards chondrocytes were compared with this list. Principal component analysis (PCA) with Pearson product-moment correlation was performed to compute correlations between the expression profiles.

Pathway analysis

Using sets of probes emerging from PCA, a search for relevant KEGG pathways was performed using the DAVID® Knowledgebase, a publicly available bioinformatics tool for functional annotation (http://david.abcc.ncifcrf.gov).

Quantitative real-time polymerase chain reaction (qPCR)

RNA was transcribed into cDNA using the First Strand cDNA Synthesis kit for qPCR (Roche Diagnostics) according to the manufacturer's protocol. Specific primer sets (available on request) were designed to amplify aggrecan (ACAN), pannexin 3 (PANX3), epiphycan (EPYC), collagen type II (COL2), and type X (COL10), SRY-box 9 (SOX9), WNT11, lymphoid enhancer-binding factor 1 (LEF1), Gremlin 1 (GREM1). β_2-Microglobulin, and glyceraldehyde 3-phosphate dehydrogenase (GAPDH) were used as housekeeping genes. Based on the microarray data, the

expression of these housekeeping genes was stable during differentiation of hfMSCs. In order to test donor inter-variation, differentiated MSCs isolated from other fetal donors were used for qPCR analysis as well.

All PCR reactions were performed in triplicate with 5 ng cDNA and according to the manufacturer's protocol of the iQ™ SYBR® Green Kit (Biorad) in a final volume of 25 µl. The cDNA was amplified using the following thermal cycling conditions: one cycle at 50°C for 2 min and 95°C for 10 min, followed by 40 cycles of 15 s at 95°C and 1 min at 56°C using the mIQ Single-Color—Real-Time PCR System (BioRad Laboratories, Hercules, California, USA). Fluorescence spectra were recorded and the threshold cycle number (Ct) was calculated using the accompanying mIQ-software. For each time point mean Ct was calculated and from this value the fold difference in expression between undifferentiated hfMSCs and differentiating cells using the $2^{-\Delta\Delta Ct}$ method was calculated essentially as described by Schmittgen and Livak, 2008 using β_2-Microglobulin as a reference. For visualization, this value was log-transformed.

Results

Chondrogenic differentiation by hfMSCs

Evaluation of protein and mRNA expression

Pellet cultures were used to induce chondrogenic differentiation of hfMSCs and samples were collected at 1, 2, 3, 4 and 5 weeks of culture. Immunohistological evaluation showed an increasing expression of cartilage markers with time and a gradual morphological change from stem cells to mature and hypertrophic chondrocytes (figure 1). The mean diameter of the pellets increased with time, as well as the amount of glycosaminoglycans, a major constituent of the cartilaginous extracellular matrix. Immunofluorescent staining for collagen type II demonstrated the presence of chondrocytes after 1 week of pellet culture. The expression of collagen type II increased over time. Hypertrophic chondrocytes were first detected after 3 weeks, as evidenced by immunohistochemical staining for collagen type X. These collagen type 10 positive cells were located in a discrete ring-like zone surrounded by collagen type 2 positive chondrocytes. In all stages of differentiation, the chondrogenic core of the pellets was surrounded by a thin layer of two to three undifferentiated cells (figure 1).

From each time point RNA was isolated and subjected to microarray analysis. Changes in gene expression of a subset of genes consisting of both established marker genes for chondrogenesis and differentially expressed genes identified by microarray analysis were validated using qPCR

(figure 2). In concordance with the observations of immunohistological markers of chondrogenesis, microarray data and qPCR showed time-dependent increases in the expression of the cartilage markers collagen type II, and type X, SOX9, and aggrecan mRNA. To further extend this analysis, we randomly selected 7 genes (pannexin 3, epiphycan, WNT11, LEF1, gremlin 1, Dickkopf 1, matrilin) that showed marked regulation over time based on microarray analysis. Again, qPCR demonstrated a strong correlation between the expression patterns revealed by both techniques (results for 5 of these genes are shown in figure 2E-I), providing further support for the robustness of our dataset. Repeating the qPCR analysis using RNA isolated from other fetal donors of MSCs that were stimulated to undergo chondrogenic differentiation rendered similar gene expression patterns as observed in this study (data not shown).

Principal component analysis and KEGG pathway analysis

The sequential changes that occur during chondrogenic differentiation in the hfMSC model were studied with bioinformatics analysis of the microarray data. Using principal component analysis, three components were found to explain 99.6% of the variance within our dataset (figure 3.A). The factor loadings in figure 3.B show that component 1 describes a general level of gene expression, as expected. Component 2 shows to what extent gene expression changed with time during chondrogenic differentiation and

Figure 1

Expression of (A) glycosaminoglycans visualized by toluidine blue staining, (B) collagen type II fluorescence, and (C) collagen type X immunohistochemistry (brown) during 5 weeks of chondrogenic differentiation of hfMSCs to chondrocytes. The top panel shows a magnification of the pellet cultures at week 1 and week 5 stained by toluidin blue demonstrating the change in cell morphology and the deposition of the extracellular matrix. The insets in panel B show higher magnifications of collagen type II positive chondrocytes.

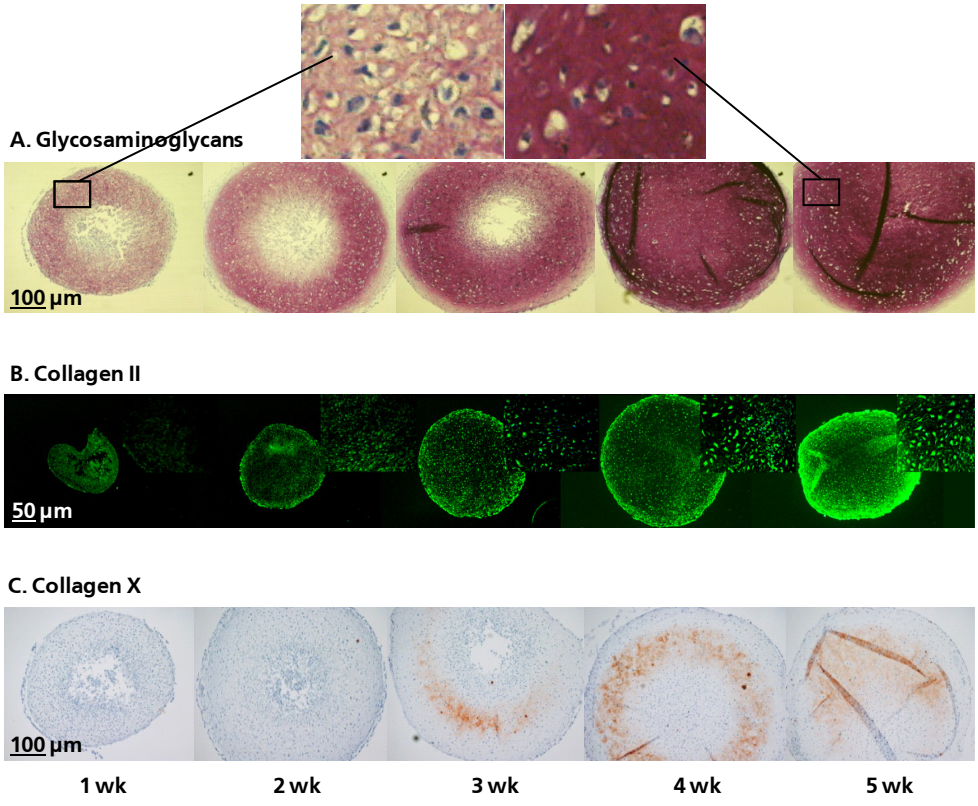

Figure 2

Correlation between qPCR and microarray expression data for (A) aggrecan, (B) collagen II, (C) collagen X, (D) SOX9, (E) pannexin 3, (F) epiphycan, (G) WNT11, (H) LEF1, and (I) gremlin 1 during 5 weeks of chondrogenic differentiation of hfMSCs. qPCR data are expressed as delta delta CT values corrected for the housekeeping gene β2-microglobulin. The primary y-axis (left) indicates the qPCR results as normalized fold expression on a log-scale. The secondary y-axis (right) indicates the microarray analysis results as least square means (lsm).

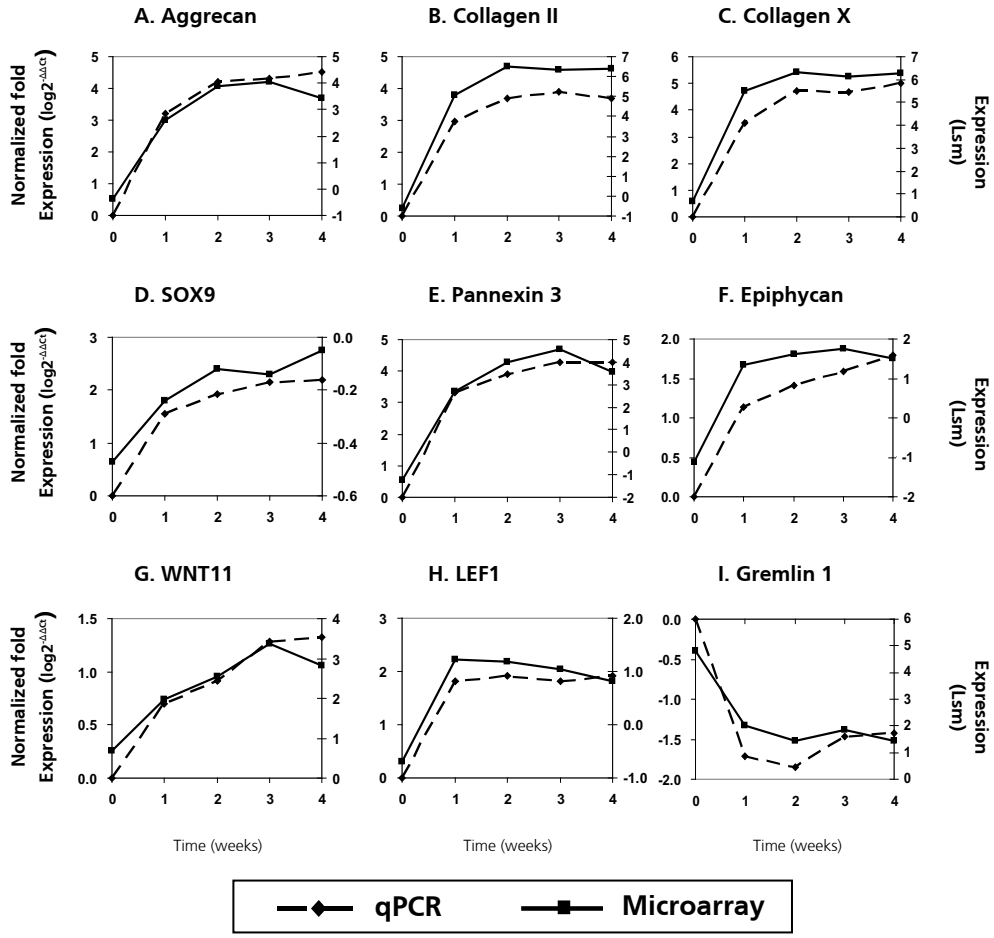

Figure 3

Gene selection based on principal component analysis. A) variance explained by components 1-6 from principal component analysis. B) principal components 1, 2, and 3 as expression profiles. C) selection of probes based on their factor 2 and 3 scores. D) scatterplot view of gene data in respect to their correlation (factor score) to prinicpal components 2 and 3. Subgroups 1, 2, 3, and 4 are represented by blue, green, yellow, and pink dots, respectively. Side-placed graphs depict the gene expression profiles for genes found in the four subgroups.

A. Variance explained by PCA

Component	Variance (%)	Cumulative variance (%)
1	95.16	95.16
2	3.24	98.40
3	1.15	99.55
4+5+6	0.45	100

B. Principal components

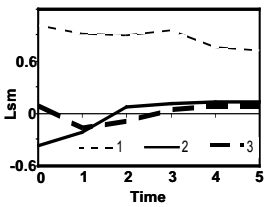

C. Subgroup definitions

Subgroup	Factor 2 score	Factor 3 score	Nº. of probes	Sign. probes
1	≤-3.29		149	146
2	≥3.29		118	105
3	<-3.29	≤-3.29	135	49
4	>3.29	≥-3.29	64	15

D. Expression profiles

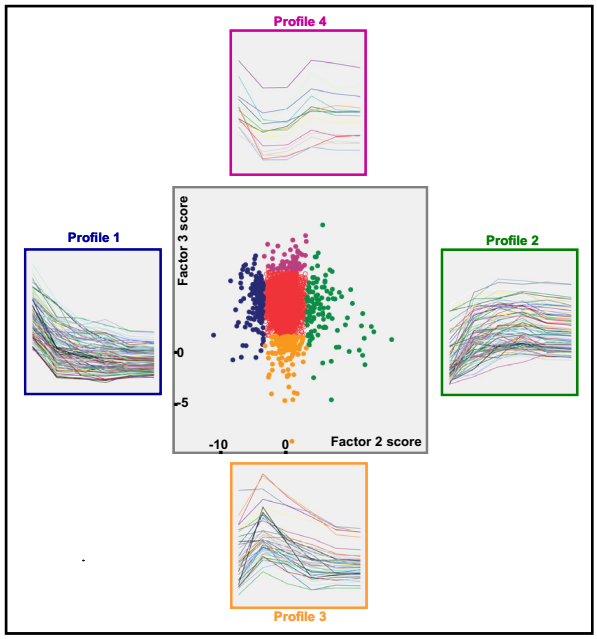

component 3 signifies whether there was an additional, short term elevation or dip in expression around 2 to 3 weeks of differentiation. Since components 2 and 3 were most likely to contain genes associated with the loss of stem cell characteristics or the gain of a chondrocyte phenotype, we focused on those components.

Using the ±3.29 cut-off in combination with a 5% significance test, we distinguished four subgroups of probes. The precise definitions and the resulting numbers of these subgroups are given in figure 3.C. The scatter plot in figure 3.D illustrates that the numbers of probes in subgroups 1 and 2 are much larger than the 9 probes (0.05%) that would have been expected under purely random selection. Moreover, in these two subgroups nearly all probes in the first selection are significant at the 5% level, suggesting that the number of false discoveries in these two groups is quite small. More noise is presumably present in the smaller subgroups 3 and 4 based on factor 3 scores.

The profiles of the selected probes demonstrate that subgroup 1 containing the largest number of probes (n=146) describes a peak of expression on t_0 followed by a decrease in expression thereafter. In contrast, the second largest subgroup of probes (n=105) in profile 2 demonstrates increasing expression levels from t_0 onward. The smaller subgroups 3 and 4 demonstrate lower levels of expression with profile 3 (n=49) showing a short-term increase in expression at t_1 followed by decreases thereafter and profile 4 (n= 15) displaying a short-term expression dip between t_1-t_2.

A total of 83 out of 315 probes could not be annotated and was discarded from further analysis. The remaining 232 probes that could be matched to genes (supplementary table 1) were used to identify 9 KEGG pathways that were significantly associated with chondrogenic differentiation and contained 39 genes. (figure 4). Some genes were present solely in one pathway (n= 23), but others were found in 2 (n= 6) or 3 (n= 10) pathways (table 1). Three functional groups of genes were recognized: 1) growth factor (GF) and GF-related genes; 2) genes associated with the extracellular matrix; and 3) genes associated with signal transduction, cell cycle, and cell survival. In supplementary table 2, we have listed the top hits of upregulated genes as identified by the microarray analysis at each time point compared to undifferentiated hfMSCs.

Figure 4

KEGG signaling pathways significantly associated with chondrogenic differentiation of hfMSCs. For each pathway, genes showing the same distinct expression profile during 5 weeks of chondrogenic differentiation are depicted as groups.

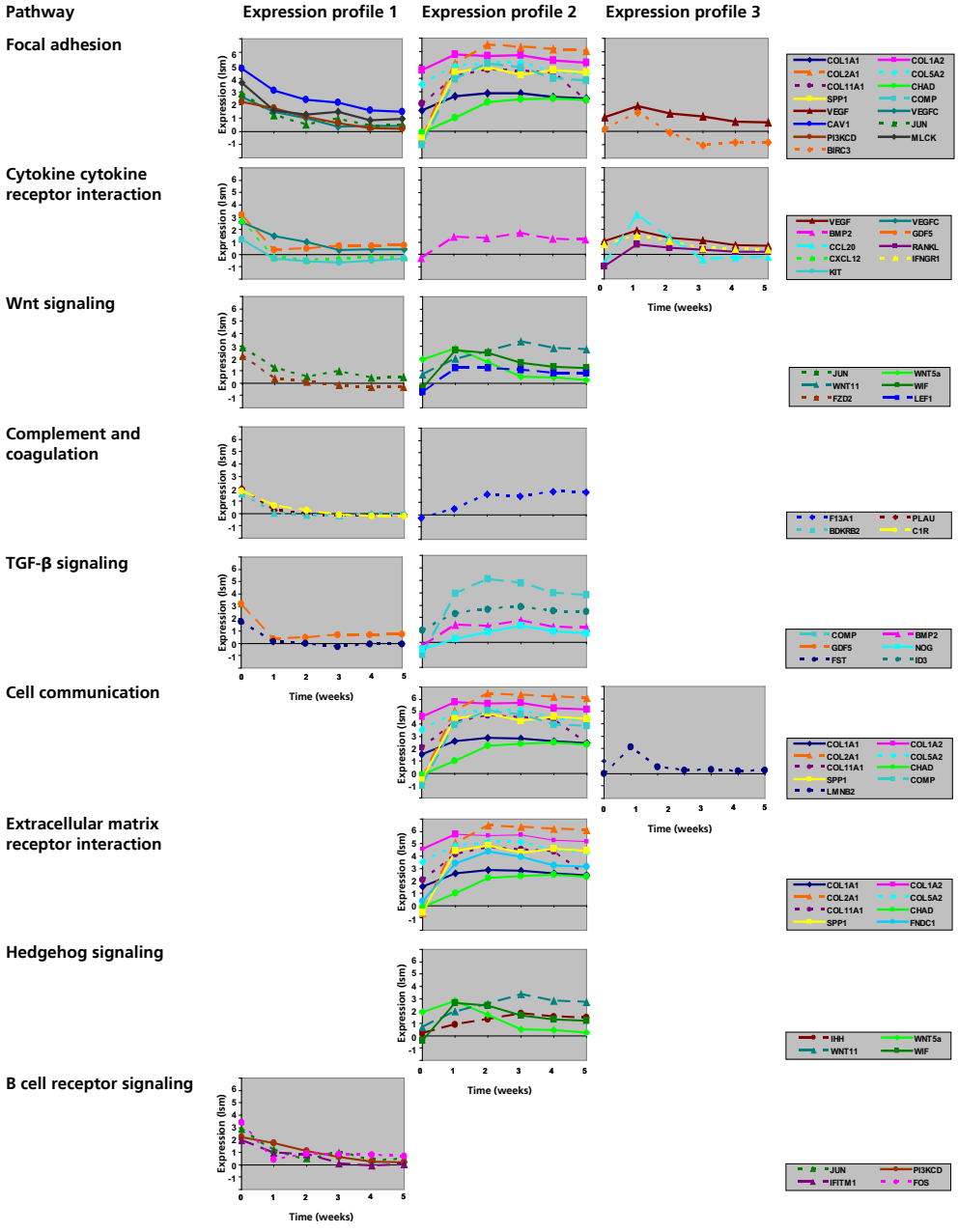

Gene expression fingerprinting for cartilage subtype

Histological and gene expression analyses showed that the differentiating hfMSCs acquire a hyaline cartilage phenotype. Two major types of hyaline cartilage can be distinguished, namely articular and epiphyseal cartilage. In order to serve as a model for the epiphyseal growth plate, differentiating hfMSCs should obtain a growth plate signature. To test this, we compared the expression profiles of the differentiating hfMSCs with previously established profiles of human articular and growth plate cartilage (AC and GP, respectively, Leijten *et al.*, in preparation). In a three-dimensional schematic representation, samples of AC and GP plot in two different groups (figure 5). As expected, AC, GP, and undifferentiated hfMSCs (hMSC_t0) plotted as distinct entities in a three-dimensional space. As differentiation progressed, the expression profile of the hfMSCs changed, and the differentiating chondrocytes gradually acquired a fingerprint resembling GP, but not AC. This analysis demonstrated that the hfMSCs differentiating towards chondrocytes acquired a GP cartilage-like phenotype.

Figure 5

Three-dimensional overviews of gene expression data in respect to their correlation (factor score) to principal components 1, 2, and 3. Red dots, samples of articular cartilage; Green dots, samples of growth plates; Blue dots, differentiation time-range of hfMSCs (t0, undifferentiated hfMSCs; t5, mature chondrocytes). Dots indicate the mean factor score for all genes on the Affymetrix chip on the three principal components for one cartilage sample. Clouds represent the spread around the mean factor score in three dimensions.

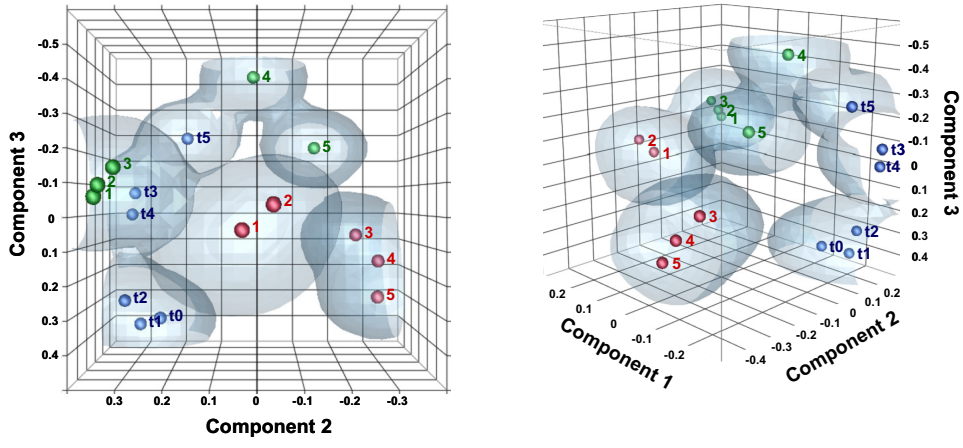

Discussion

The present study was conducted in order to determine whether fetal bone marrow-derived MSCs are a representative human model for studying processes taking place in the epiphyseal growth plate and to identify associated signaling pathways. It has been reported that human bone marrow-derived MSCs display a better chondrogenic differentiation capacity than those derived from other sources, with fetal being superior over adult MSCs (6). Consequently, it seems appropriate to use fetal bone marrow-derived MSCs as a model for chondrogenesis. However, fetal MSCs are not easily obtained, due to ethical and legal considerations, and as a consequence, adult bone marrow-derived MSCs have been used in many previous studies (11-18).

Chondrogenic differentiation occurred in our *in vitro* model, as illustrated by the progressive increase in expression of the chondrocyte markers collagen type II and X and the cartilaginous matrix constituent glycosaminoglycan over time. Interestingly, hypertrophic differentiation as evidenced by an increase in cell size and positive staining for collagen 10 was only observed in a discrete zone of the pellet which was surrounded at both sites by chondrocytes positive for collagen type 2.

Further confirmation of chondrogenesis was obtained by analysis of mRNA expression of cartilage markers, which, in addition, also validated our microarray results. Similar gene expression patterns were obtained during chondrogenic differentiation of fetal MSCs derived from other donors. This suggested that the selected 22-weeks old fetal MSC-donor was representative for fetal bone marrow in general.

Matrix mineralization was not observed after 5 weeks of differentiation, suggesting that the matrix was not ready for mineralization or that environmental stimuli necessary to induce this process were absent.

Microarray analysis generated a multidimensional dataset of differentially expressed genes for each time point. Several methods for analyzing such complex data have been reported, many based on presence/absence analysis, which starts with the list of differentially expressed genes and applies a strict but arbitrary cut-off for differential expression of individual genes (13;18). Misinterpretation of the data can easily occur, since genes are assumed to be independent, whereas it is more likely that sets of correlated genes play a role in complex biological processes (19). Genes that are not considered differentially expressed, but that do play a role in important signaling pathways, may be wrongfully eliminated. Another analysis strategy applied by many groups is to report on *a priori* selected pathway(s) of interest, thereby disregarding the relative importance of this pathway in view of other potentially co-regulated or interacting pathways.

Alternatively, we have applied PCA with restrictive criteria as a statistical selection method for identification of gene expression profiles associated with the acquisition of chondrocyte characteristics or the loss of a stem cell phenotype. Since biological replicates were not included in this study, such a stringent approach was necessary in order to minimize potentially false-positive results.
The gene expression data generated with this analytic approach are consistent with previous reports on *in vitro* cartilage formation by adult mesenchymal stem cells. We therefore conclude that PCA is a suitable and unbiased analysis tool for data reduction in multidimensional and complex microarray experiments. Using this method, 232 genes were identified to be significantly associated with chondrogenic differentiation, 39 of which were present in 9 significantly enriched KEGG pathways. These 39 genes could be classified in three major functional groups that are discussed in the following sections.

Growth factor (GF) and GF-related genes

Growth factors from the transforming growth factor β (TGF-β), Wnt, Hedgehog and VEGF families have been recognized as major regulators of endochondral bone formation in embryos and postnatally (20;21). Expression of some members of these families changed over time in our *in vitro* model suggesting their involvement in chondrocyte differentiation from fhMSCs.
BMP2 and its downstream effector ID3 are upregulated early in differentiation consistent with previous reports on the importance of BMP signaling in chondrogenesis (22;23). Growth and differentiation factor 5 (GDF5), previous reported as stimulator of chondrocyte proliferation (24), was highly expressed at the earliest time point observed and downregulated thereafter. A similar expression profile was found for the BMP inhibitor follistatine (FST) that was previously shown to be expressed by proliferative, but not by hypertrophic chondrocytes (25).
Previous *in vitro* studies have demonstrated that BMP2 interacts with Wnt and hedgehog family members and their downstream effectors, indicating that functional crosstalk between regulatory pathways occurs during chondrogenesis (23;26). Such interactions may have taken place in our *in vitro* model as well, since several genes out of the Wnt and Hedgehog family were affected during differentiation, e.g. WNT5a, WNT11, FZD2, WIF1 and IHH. IHH expression reached a maximum after 3 weeks of differentiation, a time point at which the first collagen type X positive hypertrophic chondrocytes were detected using immunohistochemistry. IHH is recognized as an important regulator of hypertrophic chondrocyte differentiation.
The superfamily of cytokines was another major group of regulatory factors for which involvement in chondrogenesis was suggested. Several genes in this group were changing

significantly over time, e.g. CXCL12, CCL20, interferon-γ (IFN-γ), IFN-γ receptor IFNGR1, interferon-induced transmembrane protein 1 (IFITM1) and the cytokine RANKL (receptor activator for nuclear factor κ B ligand). To our knowledge a role for CCL20, IFITM1, IFN-γ and its receptor IFNGR1 in chondrogenesis has not been described before.
Vascular endothelial growth factors (VEGF and VEGFC), originally described to promote epiphyseal vascularization prior to endochondral ossification, also regulate *in vitro* chondrogenesis (27-29). Both the expression of VEGF and VEGFC were significantly changing at early time points in our model.

Genes associated with the extracellular matrix

Progression of chondrogenic differentiation depends on the coordinated expression of ECM components and on cell-matrix interactions (20). Expression of several genes involved in focal adhesion, cell-matrix communication, ECM receptor interaction and matrix remodeling changed significantly over time in our *in vitro* model of chondrogenesis.
The expression of cartilaginous ECM proteins, such as collagens (COL1A1, COL1A2, COL2A1, COL5A2, COL11A1), chondroadherin (CHAD), cartilage oligomeric matrix protein (COMP), secreted phosphoprotein 1 (osteopontin, SPP1), and fibronectin type III (FNDC1), was upregulated. Apart from a structural role in the extracellular matrix, FNDC1, SPP1 and CHAD also function as integrin ligands and regulate cell-matrix signaling by binding to the cell surface plasma membrane protein integrinT. Aggregation of integrins in focal adhesions is induced by activity of myosin light chain kinase (MLCK) (30). Upon ligand-integrin binding, signaling complexes are activated that mediate downstream effectors of integrin signaling such as phosphoinositide-3-kinase (PI3K) (31), thereby stimulating cell proliferation (32). We observed early downregulation of integrin signaling-related proteins such as PI3K and MLCK.
Members of the complement and coagulation family of proteins were expressed during *in vitro* chondrogenic differentiation. Coagulation factor XIII (F13A1) expression was upregulated, while other genes like complement component I (C1R), urokinase-type plasminogen activator (PLAU) and bradykinin receptor B2 (BDKRB2) were downregulated during differentiation in our model. These proteins are associated with matrix mineralization (33-35) or matrix degradation in the growth plate (36-38).

Genes associated with signal transduction, cell cycle, and cell survival

Based on differential expression, several genes involved in the regulation of cell survival and proliferation and signal transduction were identified in our *in vitro* model of chondrogenesis. Caveolin 1 (CAV1), a multifunctional scaffolding protein located at cell surface caveolae, regulates TGF, Wnt, cytokine and VEGF signaling by modulating their downstream signaling cascades such as the JAK/STAT, β-catenin/LEF1, MAPK/ERK and PI3K/AKT signaling pathways (39-42). The anti-apoptotic baculoviral IAP repeat containing 3 (BIRC3) gene has been shown to increase the survival of cultured human chondrocytes (43). Phosphoinositide-3-kinase (PI3K), proto-oncogene KIT, transcription factor JUN and FOS are all associated to the regulation of cell proliferation (44;45). Expression of the nuclear envelope protein lamin B2 (LMNB2) was first upregulated and later in differentiation downregulated in our model. Constantinescu et al suggested a role for LMNB2 in suppressing differentiation of undifferentiated embryonic stem cells (46).

Conclusion

Many genes identified in this study were previously reported in association with chondrogenesis, validating the robustness of differentiating hfMSC as a model for cartilage formation. The implication of bradykinin and IFN-γ signaling, CCL20, and KIT are novel findings. Discrepancies between our results and reports by others may rely on differences between the source, and chondrogenic capacity of MSCs used, the experimental conditions for inducing chondrogenesis, and the gene expression analysis methods (13;14;17). Developmental genes essential for chondrogenic differentiation (e.g. SOX genes, IGF-I) were not identified, in line with other reports (15). Marginal changes in the expression of these genes may be sufficient for inducing major effects, but too subtle to be detected by most gene expression analysis methods, including PCA. Alternatively, changes occurring within the first days of differentiation may have been unnoticed due to the chosen time interval of analysis.

This study has demonstrated for the first time that bone marrow-derived hfMSCs acquire an epiphyseal GP-, rather than an AC-like gene expression signature during differentiation towards chondrocytes. This conclusion is based on comparison of expression profiles of the differentiating hfMSCs with human growth plate cartilage and human articular cartilage. These findings confirm the growth plate-like nature of the differentiating fhMSCs, indicating its validity as an alternative model for the human epiphyseal growth plate. Although a native growth plate is present in rodent animal models, these growth plates are not fully representative for the human growth plate particularly in puberty. The *in vitro* model developed in this study can potentially be used as an alternative for animal models. It is readily accessible

for genetic manipulation and might be used for unraveling the molecular mechanisms underlying growth regulation in the human epiphyseal plate during puberty. As such it may find its use in the development of novel treatment strategies for various growth disorders aimed at intervening in growth plate maturation and fusion

Acknowledgements

This work was supported by a grant from the European Society for Paediatric Endocrinology-Research Unit and by grants from ZonMW, the Netherlands Organization for Health Research and Development, to S.A. van Gool (grant number 920-03-392) and J.A.M. Emons (grant number 920-03-358) and a grant from the Deutsche Forschungsgemeinschaft to G. Rappold (Ra380/12-1). The authors gratefully acknowledge the TeRM Smart Mix Program of the Netherlands Ministry of Economic Affairs and the Netherlands Ministry of Education, Culture and Science.

Reference List

1 Chagin AS, Savendahl L: Estrogens and growth: review. Pediatr Endocrinol Rev 2007;4:329-334.

2 Nilsson O, Chrysis D, Pajulo O, Boman A, Holst M, Rubinstein J, Martin RE, Savendahl L: Localization of estrogen receptors-alpha and -beta and androgen receptor in the human growth plate at different pubertal stages. J Endocrinol 2003;177:319-326.

3 Vidal O, Lindberg MK, Hollberg K, Baylink DJ, Andersson G, Lubahn DB, Mohan S, Gustafsson JA, Ohlsson C: Estrogen receptor specificity in the regulation of skeletal growth and maturation in male mice. Proc Natl Acad Sci U S A 9-5-2000;97:5474-5479.

4 Smith EP, Boyd J, Frank GR, Takahashi H, Cohen RM, Specker B, Williams TC, Lubahn DB, Korach KS: Estrogen resistance caused by a mutation in the estrogen-receptor gene in a man. N Engl J Med 20-10-1994;331:1056-1061.

5 Pelttari K, Steck E, Richter W: The use of mesenchymal stem cells for chondrogenesis. Injury 2008;39 Suppl 1:S58-S65.

6 Bernardo ME, Emons JA, Karperien M, Nauta AJ, Willemze R, Roelofs H, Romeo S, Marchini A, Rappold GA, Vukicevic S, Locatelli F, Fibbe WE: Human mesenchymal stem cells derived from bone marrow display a better chondrogenic differentiation compared with other sources. Connect Tissue Res 2007;48:132-140.

7 in 't Anker PS, Noort WA, Scherjon SA, Kleijburg-van der Keur C, Kruisselbrink AB, van Bezooijen RL, Beekhuizen W, Willemze R, Kanhai HH, Fibbe WE: Mesenchymal stem cells in human second-trimester bone marrow, liver, lung, and spleen exhibit a similar immunophenotype but a heterogeneous multilineage differentiation potential. Haematologica 2003;88:845-852.

8 Heinrichs C, Yanovski JA, Roth AH, Yu YM, Domene HM, Yano K, Cutler GB, Jr., Baron J: Dexamethasone increases growth hormone receptor messenger ribonucleic acid levels in liver and growth plate. Endocrinology 1994;135:1113-1118.

9 Dai M, Wang P, Boyd AD, Kostov G, Athey B, Jones EG, Bunney WE, Myers RM, Speed TP, Akil H, Watson SJ, Meng F: Evolving gene/transcript definitions significantly alter the interpretation of GeneChip data. Nucleic Acids Res 2005;33:e175.

10 Chu TM, Weir B, Wolfinger R: A systematic statistical linear modeling approach to oligonucleotide array experiments. Math Biosci 2002;176:35-51.

11 Djouad F, Delorme B, Maurice M, Bony C, Apparailly F, Louis-Plence P, Canovas F, Charbord P, Noel D, Jorgensen C: Microenvironmental changes during differentiation of mesenchymal stem cells towards chondrocytes. Arthritis Res Ther 2007;9:R33.

12 Larson BL, Ylostalo J, Prockop DJ: Human multipotent stromal cells undergo sharp transition from division to development in culture. Stem Cells 2008;26:193-201.

13 Mrugala D, Dossat N, Ringe J, Delorme B, Coffy A, Bony C, Charbord P, Haupl T, Daures JP, Noel D, Jorgensen C: Gene Expression Profile of Multipotent Mesenchymal Stromal Cells: Identification of Pathways Common to TGFbeta3/BMP2-Induced Chondrogenesis. Cloning Stem Cells 28-1-2009.

14 Phinney DG, Prockop DJ: Concise review: mesenchymal stem/multipotent stromal cells: the state of transdifferentiation and modes of tissue repair--current views. Stem Cells 2007;25:2896-2902.

15 Sekiya I, Vuoristo JT, Larson BL, Prockop DJ: In vitro cartilage formation by human adult stem cells from bone marrow stroma defines the sequence of cellular and molecular events during chondrogenesis. Proc Natl Acad Sci U S A 2-4-2002;99:4397-4402.

16 Sekiya I, Larson BL, Smith JR, Pochampally R, Cui JG, Prockop DJ: Expansion of human adult stem cells from bone marrow stroma: conditions that maximize the yields of early progenitors and evaluate their quality. Stem Cells 2002;20:530-541.

17 Shahdadfar A, Fronsdal K, Haug T, Reinholt FP, Brinchmann JE: In vitro expansion of human mesenchymal stem cells: choice of serum is a determinant of cell proliferation, differentiation, gene expression, and transcriptome stability. Stem Cells 2005;23:1357-1366.

18 Ylostalo J, Smith JR, Pochampally RR, Matz R, Sekiya I, Larson BL, Vuoristo JT, Prockop DJ: Use of differentiating adult stem cells (marrow stromal cells) to identify new downstream target genes for transcription factors. Stem Cells 2006;24:642-652.

19 Goeman JJ, Buhlmann P: Analyzing gene expression data in terms of gene sets: methodological issues. Bioinformatics 15-4-2007;23:980-987.

20 DeLise AM, Fischer L, Tuan RS: Cellular interactions and signaling in cartilage development. Osteoarthritis Cartilage 2000;8:309-334.

21 Zelzer E, Olsen BR: Multiple roles of vascular endothelial growth factor (VEGF) in skeletal development, growth, and repair. Curr Top Dev Biol 2005;65:169-187.

22 De Luca F, Barnes KM, Uyeda JA, De-Levi S, Abad V, Palese T, Mericq V, Baron J: Regulation of growth plate chondrogenesis by bone morphogenetic protein-2. Endocrinology 2001;142:430-436.

23 Minina E, Wenzel HM, Kreschel C, Karp S, Gaffield W, McMahon AP, Vortkamp A: BMP and Ihh/PTHrP signaling interact to coordinate chondrocyte proliferation and differentiation. Development 2001;128:4523-4534.

24 Buxton P, Edwards C, Archer CW, Francis-West P: Growth/differentiation factor-5 (GDF-5) and skeletal development. J Bone Joint Surg Am 2001;83-A Suppl 1:S23-S30.

25 Funaba M, Ogawa K, Murata T, Fujimura H, Murata E, Abe M, Takahashi M, Torii K: Follistatin and activin in bone: expression and localization during endochondral bone development. Endocrinology 1996;137:4250-4259.

26 Tuan RS: Cellular signaling in developmental chondrogenesis: N-cadherin, Wnts, and BMP-2. J Bone Joint Surg Am 2003;85-A Suppl 2:137-141.

27 Bluteau G, Julien M, Magne D, Mallein-Gerin F, Weiss P, Daculsi G, Guicheux J: VEGF and VEGF receptors are differentially expressed in chondrocytes. Bone 2007;40:568-576.

28 Maes C, Stockmans I, Moermans K, Van Looveren R, Smets N, Carmeliet P, Bouillon R, Carmeliet G: Soluble VEGF isoforms are essential for establishing epiphyseal vascularization and regulating chondrocyte development and survival. J Clin Invest 2004;113:188-199.

29 Mayer H, Bertram H, Lindenmaier W, Korff T, Weber H, Weich H: Vascular endothelial growth factor (VEGF-A) expression in human mesenchymal stem cells: autocrine and paracrine role on osteoblastic and endothelial differentiation. J Cell Biochem 1-7-2005;95:827-839.

30 Clark K, Langeslag M, Figdor CG, van Leeuwen FN: Myosin II and mechanotransduction: a balancing act. Trends Cell Biol 2007;17:178-186.

31 Howe A, Aplin AE, Alahari SK, Juliano RL: Integrin signaling and cell growth control. Curr Opin Cell Biol 1998;10:220-231.

32 Ulici V, Hoenselaar KD, Gillespie JR, Beier F: The PI3K pathway regulates endochondral bone growth through control of hypertrophic chondrocyte differentiation. BMC Dev Biol 2008;8:40.

33 Johnson K, Hashimoto S, Lotz M, Pritzker K, Terkeltaub R: Interleukin-1 induces pro-mineralizing activity of cartilage tissue transglutaminase and factor XIIIa. Am J Pathol 2001;159:149-163.

34 Nurminskaya MV, Linsenmayer TF: Immunohistological analysis of transglutaminase factor XIIIA expression in mouse embryonic growth plate. J Orthop Res 2002;20:575-578.

35 Aeschlimann D, Mosher D, Paulsson M: Tissue transglutaminase and factor XIII in cartilage and bone remodeling. Semin Thromb Hemost 1996;22:437-443.

36 Madsen CD, Sidenius N: The interaction between urokinase receptor and vitronectin in cell adhesion and signalling. Eur J Cell Biol 2008;87:617-629.

37 Sakiyama H, Nakagawa K, Kuriiwa K, Imai K, Okada Y, Tsuchida T, Moriya H, Imajoh-Ohmi S: Complement Cls, a classical enzyme with novel functions at the endochondral ossification center: immunohistochemical staining of activated Cls with a neoantigen-specific antibody. Cell Tissue Res 1997;288:557-565.

38 Weber KT, Sun Y, Tyagi SC, Cleutjens JP: Collagen network of the myocardium: function, structural remodeling and regulatory mechanisms. J Mol Cell Cardiol 1994;26:279-292.

39 Bauer PM, Yu J, Chen Y, Hickey R, Bernatchez PN, Looft-Wilson R, Huang Y, Giordano F, Stan RV, Sessa WC: Endothelial-specific expression of caveolin-1 impairs microvascular permeability and angiogenesis. Proc Natl Acad Sci U S A 4-1-2005;102:204-209.

40 Galbiati F, Volonte D, Brown AM, Weinstein DE, Ben-Ze'ev A, Pestell RG, Lisanti MP: Caveolin-1 expression inhibits Wnt/beta-catenin/Lef-1 signaling by recruiting beta-catenin to caveolae membrane domains. J Biol Chem 28-7-2000;275:23368-23377.

41 Grande-Garcia A, del Pozo MA: Caveolin-1 in cell polarization and directional migration. Eur J Cell Biol 2008;87:641-647.

42 Jasmin JF, Mercier I, Sotgia F, Lisanti MP: SOCS proteins and caveolin-1 as negative regulators of endocrine signaling. Trends Endocrinol Metab 2006;17:150-158.

43 Gagarina V, Carlberg AL, Pereira-Mouries L, Hall DJ: Cartilage oligomeric matrix protein protects cells against death by elevating members of the IAP family of survival proteins. J Biol Chem 4-1-2008;283:648-659.

44 Hirsch E, Costa C, Ciraolo E: Phosphoinositide 3-kinases as a common platform for multi-hormone signaling. J Endocrinol 2007;194:243-256.

45 Miettinen M, Lasota J: KIT (CD117): a review on expression in normal and neoplastic tissues, and mutations and their clinicopathologic correlation. Appl Immunohistochem Mol Morphol 2005;13:205-220.

46 Constantinescu D, Gray HL, Sammak PJ, Schatten GP, Csoka AB: Lamin A/C expression is a marker of mouse and human embryonic stem cell differentiation. Stem Cells 2006;24:177-185.

Supplementary Table 1. List of genes selected with principal component analysis

Affymetrix ID	Gene code	Gene title
205856_at	SLC14A1	solute carrier family 14 (urea transporter), member 1 (Kidd blood group)
205911_at	PTHR1	parathyroid hormone receptor 1
219148_at	PBK	PDZ binding kinase
213182_x_at	CDKN1C	cyclin-dependent kinase inhibitor 1C (p57, Kip2)
206737_at	WNT11	wingless-type MMTV integration site family, member 11
203868_s_at	VCAM1	vascular cell adhesion molecule 1
218730_s_at	OGN	osteoglycin (osteoinductive factor, mimecan)
200665_s_at	SPARC	secreted protein, acidic, cysteine-rich (osteonectin)
223484_at	C15orf48	chromosome 15 open reading frame 48
206315_at	CRLF1	cytokine receptor-like factor 1
205497_at	ZNF175	zinc finger protein 175
204724_s_at	COL9A3	collagen, type IX, alpha 3
219410_at	TMEM45A	transmembrane protein 45A
218391_at	SNF8	SNF8, ESCRT-II complex subunit, homolog (S. cerevisiae)
210538_s_at	BIRC3	baculoviral IAP repeat-containing 3
201487_at	CTSC	cathepsin C
219134_at	ELTD1	EGF, latrophilin and seven transmembrane domain containing 1
212551_at	CAP2	CAP, adenylate cyclase-associated protein 2 (yeast)
206421_s_at	SERPINB7	serpin peptidase inhibitor, clade B (ovalbumin), member 7
219837_s_at	CYTL1	cytokine-like 1
210220_at	FZD2	frizzled homolog 2 (Drosophila)
207064_s_at	AOC2	amine oxidase, copper containing 2 (retina-specific)
218542_at	CEP55	centrosomal protein 55kDa
206423_at	ANGPTL7	angiopoietin-like 7
231227_at	---	Transcribed locus, strongly similar to WNT-5A protein precursor
229494_s_at	CD63	CD63 molecule
223734_at	OSAP	ovary-specific acidic protein
206614_at	GDF5	growth differentiation factor 5 (cartilage-derived morphogenetic protein-1)
205713_s_at	COMP	cartilage oligomeric matrix protein
230372_at	---	Transcribed locus, PREDICTED: similar to hyaluronan synthase 2 [Pan troglodytes]
1563724_at	SACS	Spastic ataxia of Charlevoix-Saguenay (sacsin)
203499_at	EPHA2	EPH receptor A2
1556499_s_at	COL1A1	collagen, type I, alpha 1
219230_at	TMEM100	transmembrane protein 100
206790_s_at	NDUFB1	NADH dehydrogenase (ubiquinone) 1 beta subcomplex, 7kDa
204825_at	MELK	maternal embryonic leucine zipper kinase
212565_at	STK38L	serine/threonine kinase 38 like
1554997_a_at	PTGS2	prostaglandin-endoperoxide synthase 2 (prostaglandin G/H synthase & cyclooxygenase)
204894_s_at	AOC3	amine oxidase, copper containing 3 (vascular adhesion protein 1)
203886_s_at	FBLN2	fibulin 2
203153_at	IFIT1	interferon-induced protein with tetratricopeptide repeats 1
242517_at	KISS1R	KISS1 receptor
1552340_at	SP7	Sp7 transcription factor
203963_at	CA12	carbonic anhydrase XII

1554950_at	AGC1	aggrecan 1 (chondroitin sulfate proteoglycan 1, large aggregating proteoglycan)
232451_at	---	MRNA; cDNA DKFZp564I0816 (from clone DKFZp564I0816)
227705_at	TCEAL7	transcription elongation factor A (SII)-like 7
1570574_at	GPR177	G protein-coupled receptor 177
218273_s_at	PPM2C	protein phosphatase 2C, magnesium-dependent, catalytic subunit
224735_at	CYBASC	cytochrome b, ascorbate dependent 3
239787_at	KCTD4	potassium channel tetramerisation domain containing 4
226281_at	DNER	delta-notch-like EGF repeat-containing transmembrane
218839_at	HEY1	hairy/enhancer-of-split related with YRPW motif 1
214710_s_at	CCNB1	cyclin B1
231798_at	NOG	Noggin
204595_s_at	STC1	stanniocalcin 1
209189_at	FOS	v-fos FBJ murine osteosarcoma viral oncogene homolog
203297_s_at	JARID2	Jumonji, AT rich interactive domain 2
230137_at	TMEM15	transmembrane protein 155
208078_s_at	SNF1LK	SNF1-like kinase
217989_at	DHRS8	dehydrogenase/reductase (SDR family) member 8
229125_at	ANKRD3	ankyrin repeat domain 38
205141_at	ANG	angiogenin, ribonuclease, RNase A family, 5
204712_at	WIF1	WNT inhibitory factor 1
1552960_at	LRRC15	leucine rich repeat containing 15
225155_at	SNHG5	small nucleolar RNA host gene (non-protein coding) 5
204351_at	S100P	S100 calcium binding protein P
1569372_at	TUBB2B	Tubulin, beta 2B
205097_at	SLC26A2	solute carrier family 26 (sulfate transporter), member 2
204881_s_at	UGCG	UDP-glucose ceramide glucosyltransferase
203434_s_at	MME	membrane metallo-endopeptidase (neutral endopeptidase, enkephalinase)
1568574_x_at	SPP1	Secreted phosphoprotein 1 (osteopontin, bone sialoprotein I)
206908_s_at	CLDN11	claudin 11 (oligodendrocyte transmembrane protein)
1556153_s_at	NFKBIZ	Nuclear factor of kappa light polypeptide gene enhancer in B-cells inhibitor, zeta
210643_at	TNFSF11	tumor necrosis factor (ligand) superfamily, member 11, RANKL
203305_at	F13A1	coagulation factor XIII, A1 polypeptide
213791_at	PENK	proenkephalin
242324_x_at	CCBE1	collagen and calcium binding EGF domains 1
213338_at	TMEM15	transmembrane protein 158
213139_at	SNAI2	snail homolog 2 (Drosophila)
217979_at	TSPAN13	Tetraspanin 13
215420_at	IHH	Indian hedgehog homolog (Drosophila)
229645_at	C18orf51	chromosome 18 open reading frame 51
218717_s_at	LEPREL1	leprecan-like 1
238332_at	ANKRD2	ankyrin repeat domain 29
205828_at	MMP3	matrix metallopeptidase 3 (stromelysin 1, progelatinase)
209395_at	CHI3L1	chitinase 3-like 1 (cartilage glycoprotein-39)
204337_at	RGS4	regulator of G-protein signalling 4
201939_at	PLK2	polo-like kinase 2 (Drosophila)
228844_at	SLC13A5	solute carrier family 13 (sodium-dependent citrate transporter), member 5
218468_s_at	GREM1	gremlin 1, cysteine knot superfamily, homolog (Xenopus laevis)

201467_s_at	NQO1	NAD(P)H dehydrogenase, quinone 1
224482_s_at	RAB11FIP	RAB11 family interacting protein 4 (class II)
206239_s_at	SPINK1	serine peptidase inhibitor, Kazal type 1
213492_at	COL2A1	collagen, type II, alpha 1
1552737_s_at	WWP2	WW domain containing E3 ubiquitin protein ligase 2
204162_at	KNTC2	kinetochore associated 2
213622_at	COL9A2	collagen, type IX, alpha 2
202497_x_at	SLC2A3	solute carrier family 2 (facilitated glucose transporter), member 3
206309_at	LECT1	leukocyte cell derived chemotaxin 1
1556427_s_at	LOC2210	similar to hypothetical protein
201762_s_at	PSME2	proteasome (prosome, macropain) activator subunit 2 (PA28 beta)
201795_at	LBR	lamin B receptor
209946_at	VEGFC	vascular endothelial growth factor C
210432_s_at	SCN3A	sodium channel, voltage-gated, type III, alpha
206439_at	DSPG3	dermatan sulfate proteoglycan 3
203498_at	DSCR1L1	Down syndrome critical region gene 1-like 1
202912_at	ADM	adrenomedullin
221729_at	COL5A2	collagen, type V, alpha 2
1555345_at	SLC38A4	solute carrier family 38, member 4
210095_s_at	IGFBP3	insulin-like growth factor binding protein 3
201601_x_at	IFITM1	interferon induced transmembrane protein 1 (9-27)
205483_s_at	ISG15	ISG15 ubiquitin-like modifier
1554685_a_at	KIAA119	KIAA1199
221019_s_at	COLEC12	collectin sub-family member 12
240448_at	KIAA080	KIAA0802
200790_at	ODC1	ornithine decarboxylase 1
206932_at	CH25H	cholesterol 25-hydroxylase
205352_at	SERPINI1	serpin peptidase inhibitor, clade I (neuroserpin), member 1
228640_at	---	CDNA clone IMAGE:4800096
205051_s_at	KIT	v-kit Hardy-Zuckerman 4 feline sarcoma viral oncogene homolog
204731_at	TGFBR3	transforming growth factor, beta receptor III (betaglycan, 300kDa)
221823_at	C5orf30	chromosome 5 open reading frame 30
1554736_at	ARHGAP	Rho GTPase activating protein 29
217997_at	PHLDA1	pleckstrin homology-like domain, family A, member 1
226907_at	PPP1R14	protein phosphatase 1, regulatory (inhibitor) subunit 14C
223235_s_at	SMOC2	SPARC related modular calcium binding 2
202403_s_at	COL1A2	collagen, type I, alpha 2
204469_at	PTPRZ1	protein tyrosine phosphatase, receptor-type, Z polypeptide 1
223614_at	C8orf57	chromosome 8 open reading frame 57
212850_s_at	LRP4	low density lipoprotein receptor-related protein 4
202965_s_at	CAPN6	calpain 6
223316_at	CCDC3	coiled-coil domain containing 3
200974_at	ACTA2	actin, alpha 2, smooth muscle, aorta
213293_s_at	TRIM22	tripartite motif-containing 22
222020_s_at	HNT	neurotrimin
210609_s_at	TP53I3	tumor protein p53 inducible protein 3
201739_at	SGK	serum/glucocorticoid regulated kinase

217995_at	SQRDL	sulfide quinone reductase-like (yeast)
204682_at	LTBP2	latent transforming growth factor beta binding protein 2
201195_s_at	SLC7A5	solute carrier family 7 (cationic amino acid transporter, y+ system), member 5
206764_x_at	MPPE1	metallophosphoesterase 1
213060_s_at	CHI3L2	chitinase 3-like 2
205334_at	S100A1	S100 calcium binding protein A1
209955_s_at	FAP	fibroblast activation protein, alpha
204035_at	SCG2	secretogranin II (chromogranin C)
217875_s_at	TMEPAI	transmembrane, prostate androgen induced RNA
203879_at	PIK3CD	phosphoinositide-3-kinase, catalytic, delta polypeptide
202709_at	FMOD	fibromodulin
1554737_at	FBN2	fibrillin 2 (congenital contractural arachnodactyly)
205941_s_at	COL10A	collagen, type X, alpha 1(Schmid metaphyseal chondrodysplasia)
202727_s_at	IFNGR1	interferon gamma receptor 1
226930_at	FNDC1	fibronectin type III domain containing 1
207001_x_at	TSC22D3	TSC22 domain family, member 3
206960_at	GPR23	G protein-coupled receptor 23
203666_at	CXCL12	chemokine (C-X-C motif) ligand 12 (stromal cell-derived factor 1)
204320_at	COL11A	collagen, type XI, alpha 1
203058_s_at	PAPSS2	3'-phosphoadenosine 5'-phosphosulfate synthase 2
205870_at	BDKRB2	bradykinin receptor B2
201464_x_at	JUN	v-jun sarcoma virus 17 oncogene homolog (avian)
226989_at	RGMB	RGM domain family, member B
229740_at	LOC6430	PP12104
203304_at	BAMBI	BMP and activin membrane-bound inhibitor homolog (Xenopus laevis)
218899_s_at	BAALC	brain and acute leukemia, cytoplasmic
224348_s_at	H19	H19, imprinted maternally expressed untranslated mRNA
209560_s_at	DLK1	delta-like 1 homolog (Drosophila)
222162_s_at	ADAMTS	ADAM metallopeptidase with thrombospondin type 1 motif, 1
206115_at	EGR3	early growth response 3
1562094_at	MGC269	Hypothetical protein MGC26963
216952_s_at	LMNB2	lamin B2
210948_s_at	LEF1	lymphoid enhancer-binding factor 1
1563466_at	MYLK	Myosin, light polypeptide kinase
212689_s_at	JMJD1A	jumonji domain containing 1A
205347_s_at	TMSL8	thymosin-like 8
204967_at	SHROOM	shroom family member 2
218009_s_at	PRC1	protein regulator of cytokinesis 1
212067_s_at	C1R	complement component 1, r subcomponent
1560259_at	RORA	RAR-related orphan receptor A
206432_at	HAS2	hyaluronan synthase 2
1561065_at	ANKRD6	Ankyrin repeat domain 6
1555800_at	ZNF533	zinc finger protein 533
219747_at	C4orf31	chromosome 4 open reading frame 31
1558636_s_at	ADAMTS	ADAM metallopeptidase with thrombospondin type 1 motif, 5 (aggrecanase-2)
227497_at	---	CDNA FLJ11723 fis, clone HEMBA1005314
1555527_at	COL9A1	collagen, type IX, alpha 1

202768_at	FOSB	FBJ murine osteosarcoma viral oncogene homolog B
204221_x_at	GLIPR1	GLI pathogenesis-related 1 (glioma)
204774_at	EVI2A	ecotropic viral integration site 2A
206157_at	PTX3	pentraxin-related gene, rapidly induced by IL-1 beta
202643_s_at	TNFAIP3	tumor necrosis factor, alpha-induced protein 3
234994_at	KIAA191	KIAA1913
227475_at	FOXQ1	forkhead box Q1
219334_s_at	OBFC2A	oligonucleotide/oligosaccharide-binding fold containing 2A
218986_s_at	FLJ20035	hypothetical protein FLJ20035
228382_at	FAM105	family with sequence similarity 105, member B
205523_at	HAPLN1	hyaluronan and proteoglycan link protein 1
224967_at	UGCG	UDP-glucose ceramide glucosyltransferase
213817_at	---	CDNA FLJ13601 fis, clone PLACE1010069
212900_at	SEC24A	SEC24 related gene family, member A (S. cerevisiae)
1552619_a_at	ANLN	anillin, actin binding protein
224609_at	SLC44A2	solute carrier family 44, member 2
203755_at	BUB1B	BUB1 budding uninhibited by benzimidazoles 1 homolog beta (yeast)
1555724_s_at	TAGLN	transgelin
202450_s_at	CTSK	cathepsin K (pycnodysostosis)
213861_s_at	FAM119	family with sequence similarity 119, member B
213248_at	LOC2213	hypothetical protein LOC221362
203570_at	LOXL1	lysyl oxidase-like 1
230407_at	---	Transcribed locus, strongly similar to strawberry notch homolog 1; MOP-3
209567_at	RRS1	RRS1 ribosome biogenesis regulator homolog (S. cerevisiae)
210512_s_at	VEGF	vascular endothelial growth factor
205289_at	BMP2	bone morphogenetic protein 2
203065_s_at	CAV1	caveolin 1, caveolae protein, 22kDa
203758_at	CTSO	cathepsin O
205476_at	CCL20	chemokine (C-C motif) ligand 20
207826_s_at	ID3	inhibitor of DNA binding 3, dominant negative helix-loop-helix protein
205479_s_at	PLAU	plasminogen activator, urokinase
201136_at	PLP2	proteolipid protein 2 (colonic epithelium-enriched)
203764_at	DLG7	discs, large homolog 7 (Drosophila)
209160_at	AKR1C3	aldo-keto reductase family 1, member C3 (3-alpha hydroxysteroid dehydrogenase, type II)
207977_s_at	DPT	dermatopontin
205125_at	PLCD1	phospholipase C, delta 1
207980_s_at	CITED2	Cbp/p300-interacting transactivator, with Glu/Asp-rich carboxy-terminal domain, 2
204475_at	MMP1	matrix metallopeptidase 1 (interstitial collagenase)
1556209_at	CLEC2B	C-type lectin domain family 2, member B
205830_at	CLGN	calmegin
219295_s_at	PCOLCE2	procollagen C-endopeptidase enhancer 2
205907_s_at	OMD	osteomodulin
206869_at	CHAD	chondroadherin
223836_at	KSP37	Ksp37 protein
204948_s_at	FST	follistatin
240955_at	PANX3	pannexin 3

Supplementary Table 2. List of top hits of upregulated genes at each time point with their fold change in expression compared to undifferentiated hfMSCs

TOP upregulated genes of pellets isolated at 1 week of differentiation compared to undifferentiated hfMSCs

Symbol	Gene title	Fold change
COL2A1	collagen, type II, alpha 1	48,69295
COMP	cartilage oligomeric matrix protein	29,52449
SPP1	Secreted phosphoprotein 1 (osteopontin)	29,24743
COL10A1	collagen, type X, alpha 1	26,33897
S100P	S100 calcium binding protein P	23,64239
ANKRD38	ankyrin repeat domain 38	21,03949
H19	H19, imprinted maternally expressed untranslated mRNA	20,74613
COL9A3	collagen, type IX, alpha 3	17,44117
OMD	osteomodulin	14,81684
CCL20	chemokine (C-C motif) ligand 20	14,58234
PANX3	pannexin 3	14,0997
SP7	Sp7 transcription factor	10,99764
WIF1	WNT inhibitory factor 1	7,854743
FNDC1	fibronectin type III domain containing 1	7,754044
MMP3	matrix metallopeptidase 3	7,723496

TOP upregulated genes of pellets isolated at 2 weeks of differentiation compared to undifferentiated hfMSCs

Symbol	Gene title	Fold change
COL2A1	collagen, type II, alpha 1	127,526
COMP	cartilage oligomeric matrix protein	63,39943
COL9A3	collagen, type IX, alpha 3	56,65738
COL10A1	collagen, type X, alpha 1	43,11545
S100P	S100 calcium binding protein P	39,35336
SPP1	Secreted phosphoprotein 1 (osteopontin)	38,08394
H19	H19, imprinted maternally expressed untranslated mRNA	37,46208
PANX3	pannexin 3	35,24063
OMD	osteomodulin	26,66117
ANGPTL7	angiopoietin-like 7	20,79869
AGC1	aggrecan 1 (chondroitin sulfate proteoglycan 1)	17,50114
FMOD	fibromodulin	16,41947
ANKRD38	ankyrin repeat domain 38	14,97306
FNDC1	fibronectin type III domain containing 1	14,939
SP7	Sp7 transcription factor	12,00436

TOP upregulated genes of pellets isolated at 3 weeks of differentiation compared to undifferentiated hfMSCs

Symbol	Gene title	Fold change
COL2A1	collagen, type II, alpha 1	124,5769
PANX3	pannexin 3	56,73114
COMP	cartilage oligomeric matrix protein	55,02747
COL9A3	collagen, type IX, alpha 3	52,95049
S100P	S100 calcium binding protein P	47,56261
COL10A1	collagen, type X, alpha 1	42,84764
H19	H19, imprinted maternally expressed untranslated mRNA	37,78425
SPP1	Secreted phosphoprotein 1 (osteopontin)	29,09326
OMD	osteomodulin	28,90007
ANGPTL7	angiopoietin-like 7	24,41976
AGC1	aggrecan 1 (chondroitin sulfate proteoglycan 1)	21,56025
FMOD	fibromodulin	19,79998
SMOC2	SPARC related modular calcium binding 2	18,17641
SLC13A5	solute carrier family 13 (sodium-dependent citrate transporter), member 5	16,55767
SP7	Sp7 transcription factor	14,70519

TOP upregulated genes of pellets isolated at 4 weeks of differentiation compared to undifferentiated hfMSCs

Symbol	Gene title	Fold change
COL2A1	collagen, type II, alpha 1	86,82906
COL10A1	collagen. type X, alpha 1	43,4907
COL9A3	collagen, type IX, alpha 3	31,28265
SPP1	Secreted phosphoprotein 1 (osteopontin)	30,3413
S100P	S100 calcium binding protein P	25,19413
PANX3	pannexin 3	17,31646
COMP	cartilage oligomeric matrix protein	16,64807
ANGPTL7	angiopoietin-like 7	14,37924
H19	H19, imprinted maternally expressed untranslated mRNA	13,72816
FMOD	fibromodulin	10,87799
OMD	osteomodulin	10,24159
AGC1	aggrecan 1 (chondroitin sulfate proteoglycan 1)	9,153789
CAPN6	calpain 6	8,080906
SMOC2	SPARC related modular calcium binding 2	7,830802
SLC13A5	solute carrier family 13 (sodium-dependent citrate transporter), member 5	7,085708

TOP upregulated genes of pellets isolated at 5 weeks of differentiation compared to undifferentiated hfMSCs

Symbol	Gene title	Fold change
COL2A1	collagen, type II, alpha 1	118,4129
COL10A1	collagen, type X, alpha 1	43,15333
COL9A3	collagen, type IX, alpha 3	64,24298
SPP1	Secreted phosphoprotein 1 (osteopontin)	36,69967
S100P	S100 calcium binding protein P	45,26042
PANX3	pannexin 3	36,55029
COMP	cartilage oligomeric matrix protein	49,01692
ANGPTL7	angiopoietin-like 7	24,0925
H19	H19, imprinted maternally expressed untranslated mRNA	27,29474
FMOD	fibromodulin	22,08534
OMD	osteomodulin	22,77907
AGC1	aggrecan 1 (chondroitin sulfate proteoglycan 1)	19,0998
CAPN6	calpain 6	9,836288
SMOC2	SPARC related modular calcium binding 2	16,58001
SLC13A5	solute carrier family 13 (sodium-dependent citrate transporter), member 5	13,48765